

Tridimensional late gadolinium enhancement at 3 T cardiac magnetic resonance for the evaluation of coronary venous anatomy: feasibility and findings

Realce tardío con gadolinio en resonancia magnética cardiaca de 3 T para la evaluación de la anatomía venosa coronaria: factibilidad y hallazgos

Erick Blanco Daza¹

Natalia Andrea Aldana Sepúlveda²

Nicolás Zuluaga Molina³

Ana María Patiño Isaza⁴

Natalia Sierra Prada⁵

Alejandro Zuluaga Santamaría⁶

DOI: <https://doi.org/10.53903/01212095.156>



Key words (MeSH)

Coronary vessels
Cicatrix
Magnetic resonance imaging
Cardiac imaging techniques

Palabras clave (DeCS)

Vasos coronarios
Cicatriz
Imagen por resonancia magnética
Técnicas de imagen cardiaca

Summary

Objective: Knowledge of coronary venous anatomy (CVA) has critical importance for planning and performing electrophysiological procedures such as cardiac resynchronization therapy (CRT), left ventricle and right atrium ablation therapy and catheter arrhythmia mapping. Our aim is to evaluate the feasibility and applications of cardiac magnetic resonance imaging (RMC) performed at 3T for non-invasive depiction of CVA employing a three-dimensional late gadolinium enhancement sequence (3D RTG). **Methods:** 138 consecutive patients who underwent 3T RMC were evaluated using a 3D RTG sequence over a period of one year between 2016 and 2017. Identification of different coronary venous structures as well as its relationship with myocardial fibrosis and other relevant clinical variables were recorded. Quality assessment was performed creating 3 groups (optimal, good, poor) according to visual assessment of each individual study. Association tests (Chi-square and Kruskal-Wallis) were performed. **Results:** The study included 62 women and 76 men with a median age of 48 (29-61) years. 3D RTG sequence yielded a diagnostic quality (optimal-good) for CVA evaluation in 76% of patients ($p < 0.001$). The following structures were identified (patients, %): anterior interventricular vein: 110 (79.7%), great cardiac vein: 109 (79%), posterior interventricular vein: 106 (76.8%), marginal vein: 53 patients (38.4%) and posterolateral vein: 74 (53.6%). Myocardial fibrosis was identified in 42 patients and epicardic fibrotic involvement of at least one coronary vein path was recorded on 12% of patients on this subset. Shorter acquisition periods ($p < 0.02$) and performing the study under general anesthesia ($p < 0.03$) resulted in significantly better study quality. **Conclusions:** Non-invasive CVA evaluation is feasible with 3D RTG sequence obtained at 3T RMC. This approach may offer a valuable clinical tool for electrophysiological procedural planning.

Resumen

Objetivo: El conocimiento de la anatomía venosa coronaria (AVC) tiene importancia crítica para planificar y realizar procedimientos electrofisiológicos como la terapia de resincronización cardiaca (TRC), la terapia de ablación del ventrículo izquierdo y la aurícula derecha y el mapeo de arritmias por catéter. El objetivo es evaluar la viabilidad y las aplicaciones de la resonancia magnética (RM) cardiaca realizada en 3 T para la representación no invasiva de la AVC empleando una secuencia tridimensional de realce tardío con gadolinio (RTG-3D). **Metodología:** Se evaluaron 138 pacientes consecutivos que se sometieron a RM cardiaca 3 T mediante una secuencia RTG-3D durante un año, entre 2016 y 2017. Se identificaron diferentes estructuras venosas coronarias, así como su relación con la fibrosis miocárdica, y otras variables clínicas relevantes. La evaluación de la calidad se realizó mediante tres grupos (óptimos, buenos, malos) de acuerdo con la evaluación visual de cada estudio individual. Se realizaron pruebas de asociación (Chi-cuadrado y Kruskal-Wallis). **Resultados:** El estudio incluyó 62 mujeres y 76 hombres con una edad promedio de 48 (29-61) años. La secuencia RTG-3D arrojó una calidad diagnóstica (óptima-buena) para la evaluación del AVC en el 76 % de los pacientes ($p < 0,001$). Se identificaron las siguientes estructuras (pacientes, %): vena interventricular anterior: 110 (79,7 %), gran vena cardiaca: 109 (79 %), vena interventricular posterior: 106 (76,8 %), vena marginal: 53 pacientes (38,4 %) y vena posterolateral: 74 (53,6 %).

¹Body Imaging Radiologist, Centro Oncológico de Antioquia, Quirónsalud. Medellín, Colombia. ORCID: 0000-0002-1309-139X

²Cardiovascular Radiologist CediMed Quirónsalud. Medellín, Colombia. ORCID: 0000-0002-9017-093X

³Radiology Resident Universidad Pontificia Bolivariana, CediMed, Quirónsalud. Medellín, Colombia.

⁴General Physician, Corporación Universitaria Remington. Medellín, Colombia. ORCID: 0000-0003-3586-7096

⁵General Practitioner, Universidad CES. Medellín, Colombia. ORCID: 0000-0002-9213-6049

⁶Diagnostic Radiologist CediMed Quirónsalud, professor of Radiology Universidad Pontificia Bolivariana, coordinator of Specialization in Radiology and Diagnostic Imaging UPB. Medellín, Colombia. ORCID: 0000-0002-2421-1254

Se identificó fibrosis miocárdica en 42 pacientes y se registró afectación fibrótica epicárdica de al menos un trayecto en una de las venas coronarias en el 12 % de los pacientes de este subgrupo. Los periodos de adquisición más cortos ($p < 0,02$) y la realización del estudio bajo anestesia general ($p < 0,03$) dieron como resultado una calidad del estudio significativamente mejor. **Conclusiones:** La evaluación no invasiva de la AVC es factible con la secuencia RTG-3D obtenida en 3 T RM cardiaca. Este enfoque puede ofrecer una valiosa herramienta clínica para la planificación de procedimientos electrofisiológicos.

1. Introduction

Coronary venous anatomy (CVA) is highly variable in terms of trajectory, shape and number of veins (1, 2). Therefore, its knowledge plays a key role in planning procedures and performing electrophysiological therapies including: cardiac resynchronization therapy (CRT), arrhythmia mapping, radiofrequency ablation, local drug delivery, gene therapy, and percutaneous balloon valvuloplasty (3, 4). Accurate CVA information not only expedites procedures, but also generates higher success rates (5). Currently, the most common diagnostic modality for the evaluation of CVA is coronary venous angiography, although with intrinsic risks associated with its invasive nature, such as the requirement of contrast media administration and exposure to ionizing radiation (6). Coronary computed tomography angiography (CTA) has established itself as an important tool in the noninvasive evaluation of CVA, not only because of its high temporal resolution provided by triggered images and rapid acquisition, but also because it has the ability to fuse and combine images with other modalities (angiography, CMR) creating accurate navigation maps. Similar to coronary venous angiography, cardiac CTA carries the burden of contrast media administration and exposure to ionizing radiation (5, 7-11).

CRT is an effective and recognized treatment in patients with heart failure, prolonged QRS and impaired left ventricular (LV) systolic function. Despite adequate patient selection, reports of treatment failure are found in almost one third of cases. The most accepted hypothesis associated with CRT failure involves LV lead misplacement due to variations in the course of venous anatomy and the presence of myocardial fibrosis around the selected vein (7). Therefore, recognizing that RTG RMC is currently the gold standard for the evaluation of myocardial fibrosis, recently published studies have demonstrated its ability to detect areas of scar surrounding coronary veins, allowing for proper pre-procedural selection for the LV lead implantation site, with the added advantage and benefit of creating a combination that includes CTA imaging and electroanatomic venous angiography maps creating high quality navigation maps for the electrophysiologist (12-14). Almost all published studies have been performed on 1.5 T scanners using two-dimensional RTG sequences (7, 12, 13, 15-17). To our knowledge, in the available literature on coronary venous evaluation, only the study by Kočková et al. (18) was performed with 3 T and was based on RTG sequences. RTG-3D sequences are mainly acquired on 3 T scanners and can provide an isotropic resolution of 1.4 mm, which allows multiple reformations and high-quality reconstructions to improve coronary venous visualization, as well as the creation of 3D volume rendered models. It also facilitates the evaluation of associated myocardial entities such as congenital malformations, ischemic disease and cardiomyopathies. The aim of this work is to evaluate the feasibility and relevant findings associated with the acquisition of a RTG-3D sequence performed on a 3T scanner.

2. Methodology

2.1. Subjects and RMC Protocol

A cross-sectional analytical study was performed at an Advanced Diagnostic Imaging Center in Medellín, Colombia, between January 2016 and February 2017. The study included 138 consecutive patients. It should be noted that the RTG-3D sequence is part of our institutional CMR protocol and is performed in all patients regardless of age or study indication, so the inclusion criteria applied were: 1) having an RTG-3D sequence included in the patient's study protocol and 2) study obtained on a 3 T scanner. All patients gave written informed consent and the study was approved by the Ethics Committee of the Pontifical Bolivarian University. Clinical variables-including gender, age, baseline heart rate, left ventricular ejection fraction (LVEF), requirement of general anesthesia for the study, and presumed diagnosis-were recorded from each patient's clinical history in a structured database.

Imaging was performed with a 3 T RMC scanner (Magnetom-Skyra®, Siemens Healthcare, Erlangen, Germany) equipped with a 30-element body surface receiver coil. An intravenous bolus of 0.1 mmol/kg gadobutrol (Gadovist®, Bayer-Schering, Berlin, Germany) was administered seven minutes before the start of image acquisition. The RTG-3D sequence performed is whole heart inversion recovery gradient echo pulse echo with respiratory navigation. Images were acquired in an axial plane with an isotropic voxel diameter of $1.4 \times 1.4 \times 1.4$ mm (repetition time: 789 ms, echo time: 1.34 ms, flip angle: 15° , bandwidth: 698 Hz/pixel, parallel imaging with GRAPPA technique). Initially, a short-axis inversion time (IT) scan of the mid LV short axis was performed to accurately suppress the signal from healthy myocardium. Subsequently, another TI scanner was defined for the RTG-3D sequence by adding 25-40 ms to the originally obtained TI. Patients were instructed to maintain regular shallow breathing during image acquisition. The time required for the acquisition of the RTG-3D sequence was recorded in minutes.

2.2. Processing and interpretation of CMR images

Images were transferred to our institutional PACS (Carestream® 2011, V. 11.140.17) and to an advanced segmentation tool (CMR42®, V. 5.3.4, Circle cardiovascular imaging, Alberta, Canada) for tissue characterization. Two cardiovascular radiologists with experience (> 8 years) in CMR interpretation evaluated the images in consensus. Image quality as defined by healthy myocardial signal suppression and spatial contrast resolution was classified as "optimal," "good," or "poor" (Figure 1).

To aid image interpretation, multiplanar reconstructions (MPR) were performed on the workstation (Vitrea®, model VWS-001SA

and Osirix MD® v 8.5) and also 3D maximum intensity projection MPR (Figure 2).

A systematic approach to CVA assessment was performed by recording the presence of the following structures: coronary sinus (identified in the axial plane), anterior interventricular vein (AIV), posterior interventricular vein (PIV), great coronary vein (GCV), posterolateral vein (PLV) and marginal vein (MV). We also recorded whether the patient had areas of epicardial myocardial scarring surrounding the course of any vein.

2.3 Statistical analysis

Numerical variables were described as median and interquartile range (Q1-Q3) due to non-compliance with the normality assumption assessed with the Kolmogorov-Smirnov test; qualitative variables were described as n (%). Image quality was evaluated and the percentages of visualization of coronary venous structures were estimated, as well as other clinically relevant variables according to sequence quality and their association was evaluated by Chi-square test. For the comparison of quality according to other variables such as age, heart rate, LVEF and sequence acquisition time, the Kruskal-Wallis test was used, estimating a two-tailed p value and establishing statistical significance with a p value < 0.05. In addition, a Fisher's exact test was performed to compare the performance between ASD and RMC obtained at 3 T for HCV visualization. Statistical analysis was performed using SPSS v. 24.0.

2.4. Results

We included 138 eligible patients who met the inclusion criteria and underwent a 3 T CMR study containing a RTG-3D sequence. The median age was 48 years (RIC 29-61) and 55 % were male. The most common diagnosis motivating the examination was cardiomyopathy and most patients had preserved LVEF with a median of 58.4 % (RIC 46-67 %). Other baseline clinical characteristics are presented in Table 1.

There were statistically significant differences between optimal-quality and poor quality patients, resulting in better and more frequent visualization of coronary venous anatomy ($p < 0.001$). Images in the poor-quality group were severely hampered by motion artifacts, resulting in a nondiagnostic study in the vast majority of cases. Among other variables evaluated, the use of general anesthesia resulted in statistically significantly better image quality ($p < 0.021$), as well as shorter sequence acquisition times ($p < 0.032$). The median time to sequence acquisition was 11 (IQR 8-14) minutes. There was no significant difference between image quality and any demographic factor, such as heart rate, age or LVEF.

Table 1. Baseline characteristics of the study population

Variable	Total cohort	
Age (years)*	48 (29-61)	
Male gender*	76 (55.1)	
LVEF (%)*	58.4 (46-67)	
Use of general anesthesia*	12 (8.7)	
Heart rate (beats/min)*	66 (56-74)	
Baseline diagnosis*	Healthy	20 (14.5)
	Cardiomyopathy (ischemic, non-ischemic, hypertrophic, asymmetric, non-compacted, dilated, restrictive myocardium)	44 (31.8)
	Congenital cardiomyopathy (atrial septal defect, ventricular septal defect, tetralogy of Fallot, transposition of great arteries, pulmonary artery stenosis, anomalous pulmonary venous return)	24 (17.5)
	Myocarditis (acute, chronic)	13 (9.4)
	Myocardial infarction (acute, chronic)	10 (7.2)
	Cardiac tumor (atrial myxoma, pericardial cyst, ventricular fibroma and solitary fibrous tumor of pleura)	7 (5.1)
	Pericarditis (acute, chronic)	3 (2.2)
	Other entities (Anderson-Fabry disease, amyloidosis, sarcoidosis, heart valve disease, ventricular rupture, aortic root aneurysm, aorto-atrial fistula)	17 (12.3)

Notes: *: continuous data, median IQR (interquartile range), + n (%): categorical data, LVEF: left ventricular ejection fraction.

2.5. Anatomical observations

Table 2 summarizes the data on coronary venous anatomy and their visualization rates in relation to image quality. The coronary sinus, AIV, PIV and GCV were visualized in more than 96% of patients with a study quality considered optimal or good. In contrast, in patients with a study quality considered poor, visualization of the aforementioned structures was only 27% at best. The overall visualization rates of the lateral veins of the left ventricle (observing a posterolateral or marginal vein) were 100% for studies of optimal quality, 83% for studies of good quality and only 3% for studies of poor quality.

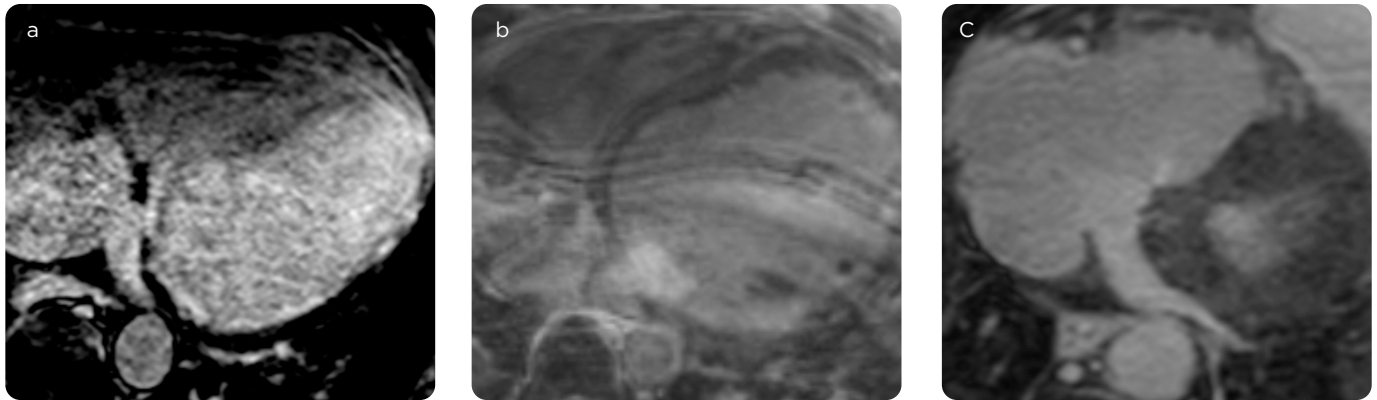


Figure 1. Quality assessment of each study defined by consensus: a) optimal, b) good and c) poor.

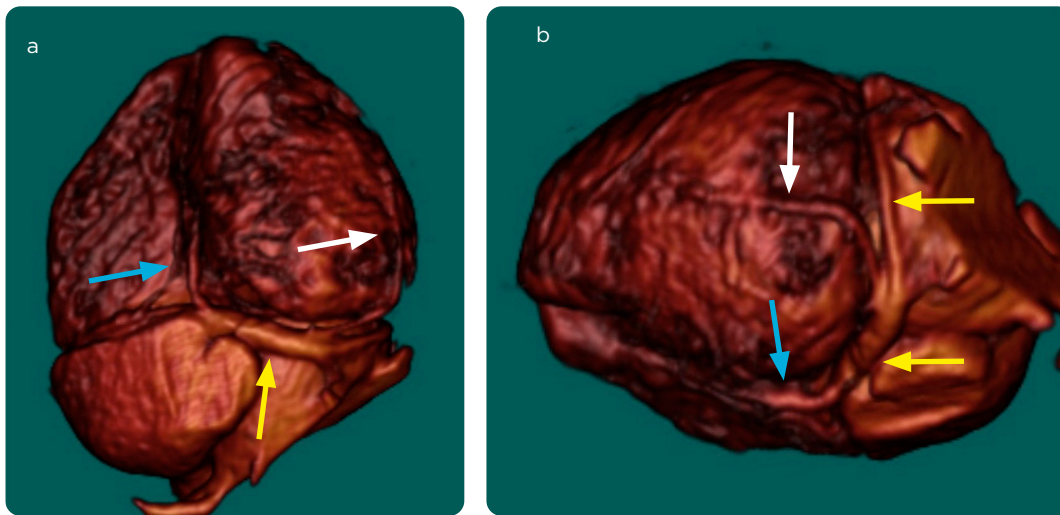


Figure 2. Reconstructions of coronary venous anatomy based on 3D-GRT. a) inferior view. b) left lateral view. Yellow arrow: coronary sinus. Blue arrow: posterior interventricular vein. Green arrow: cardiac magna vein. White arrow: left ventricular marginal vein.

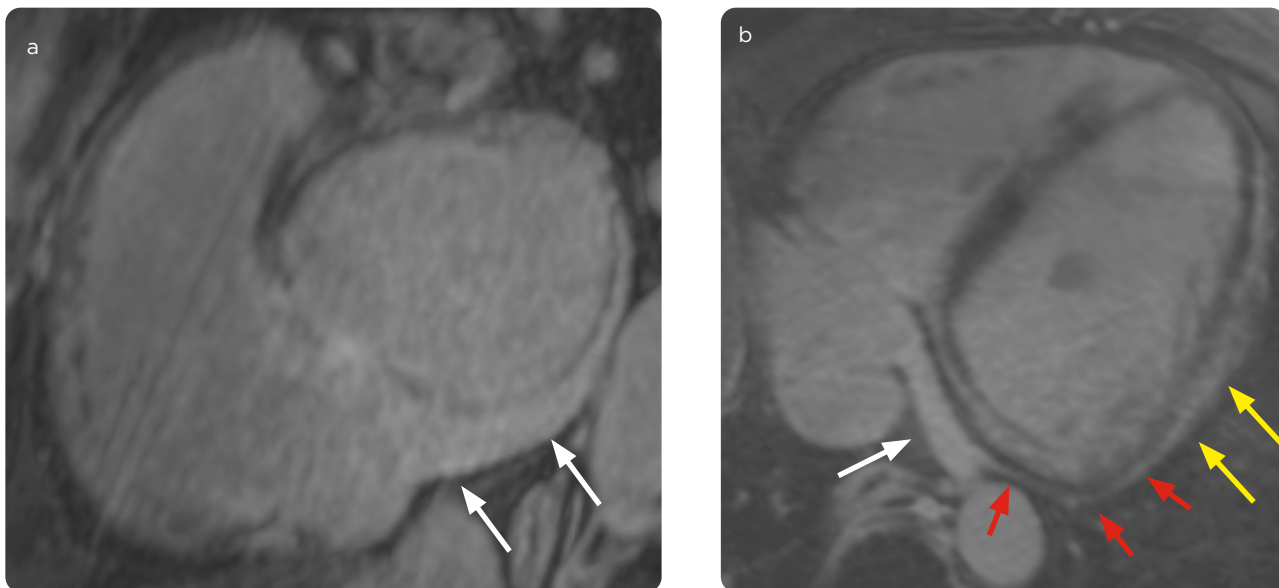


Figure 3. Coronary venous anatomy and its relationship with the areas of epicardial myocardial fibrosis based on 3D late enhancement sequence (3D-LGE) images. Multiplanar reconstructions performed from the 3D late enhancement sequence. a) Oblique short-axis reconstruction following the path of the coronary sinus (banana arrows) and b) oblique 4-chamber reconstruction following the path of the left ventricular marginal vein (red arrows) and its relationship with an extensive area of intramural and epicardial fibrosis in the lateral wall of the LV (yellow arrows).

Table 2. Association between sequence quality and visualization of coronary venous structure with clinically relevant variables

Variable	Sequence quality defined by consensus				p-value
	Optimal (27)	Good (78)	Poor (34)	Total (138)	
Coronary sinus	27 (100.0)	78 (100.0)	9 (27.3)	114 (82.6)	<0.001*
Anterior intraventricular vein	27 (100.0)	75 (96.2)	8 (24.2)	110 (79.7)	<0.001*
Great cardiac vein	27 (100.0)	76 (97.4)	6 (18.2)	109 (79.0)	<0.001*
Posterior intraventricular vein	27 (96.3)	75 (96.2)	5 (15.2)	106 (76.8)	<0.001*
Marginal vein	17 (63.0)	35 (44.9)	1 (3.0)	53 (38.4)	<0.001*
Posterolateral vein	22 (81.5)	52 (66.7)	0 (0)	74 (53.6)	<0.001*
Masculine gender	11 (40.7)	46 (59.0)	19 (57.6)	76 (55.1)	0.245*
General anesthesia n (%)	6 (22.2)	4 (5.1)	2 (6.1)	12 (8.7)	0.021*
Age. Me (IQR)	48 (39-62)	49 (28-59)	46 (24-63)	48 (29-61)	0.763 [^]
Heart rate. bpm. Me (IQR)	61 (54-70)	66.5 (56-76)	66 (59-77)	66 (56-74)	0.353 [^]
LVEF (%). Me (IQR)	61 (49-68)	58.9 (46-67)	52 (40-64.3)	58.4 (46-67)	0.188 [^]
Sequence acquisition time (min). Me (IQR)	9 (7-13)	11 (8-14)	12 (10-16)	11 (8-14)	0.037 [^]

Notes: Me (IQR): median (interquartile range), n (%): categorical data, *: chi-square test, [^]: Kruskal-Wallis test, LVEF: left ventricular ejection fraction.

2.6. Assessment of myocardial fibrosis.

Myocardial fibrosis affecting the left ventricle was identified overall in 30.4% of patients; in 69.1% it was non-ischemic, in 26.1%, ischemic and in 4.8%, mixed type fibrosis. In 12% of the patients a relationship was found between the course of a coronary vein in the left ventricle and epicardial myocardial fibrosis surrounding that area (Figure 3).

2.7. Congenital heart disease

Congenital heart disease was present in 16.7% of the sample, which included: atrial septal defect, ventricular septal defect, tetralogy of Fallot, transposition of the great arteries, pulmonary artery stenosis and anomalous pulmonary venous return. Myocardial fibrosis accompanied congenital heart defects in 34.7% of this subgroup of patients.

3. Discussion

This work demonstrates the feasibility of the RTG-3D sequence obtained with 3T to evaluate and adequately depict coronary venous anatomy. Sequences with optimal or good quality were obtained in 76% of patients, with statistically significant rates for visualization of CVA. Some points to highlight and consider from the study are discussed below: first, to the best of the authors' knowledge, this represents the largest group of patients with non-invasive CVA evaluation available in the literature, as well as the only study based on a 3T RTG-3D sequence.

CMR obtained at 3 T has evolved in recent years thanks to more refined, free-breathing (synchronized) and faster sequences (19) that allow higher resolution images to be acquired, minimizing motion artifact and field inhomogeneity. At the institution where the study was performed, more than 90% of CMRs are acquired in 3T as an institutional protocol; all studies include an RTG-3D sequence regardless of the indication of the study.

Initially, this decision was made to improve the accuracy of fibrosis assessment, but with continued use of the sequence, the authors noted the great ability of the sequence to not only provide information-quantification of fibrotic tissue, but also to clearly depict anatomic structures (venous, arterial, anatomic variants, and congenital defects) and, therefore, were the experience and motivation to conduct this study. Second, despite the high variability of visualization of coronary venous anatomy described in previous studies by Chiribiri et al. (1, 20, 21), the present work found slightly higher visualization rates using the RTG-3D sequence. Table 3 shows a comparison between these studies. Third and finally, when comparing the diagnostic performance in this work with the available results from the literature based on DSA, no statistically significant differences were found for CVA visualization between DSA and RTG-3D CMR, except for the posterior interventricular vein ($p < 0.001$), which was observed at a higher percentage (96.2%) in this work with RTG-3T CMR, compared with the percentage of visualization of the same with DSA in the study by Blendea et al. (1) of 76% (Table 4). Similar visualization rates are observed in different modalities: angiography (which is the current gold standard) and CMR obtained at 1.5 T and 3 T. These findings suggest that the RTG-3D sequence acquired at 3 T constitutes a valuable tool for the non-invasive assessment of CVA with a performance comparable to DSA, which currently remains the technique used as the gold standard. Beyond the assessment of CVA, the primary objective of the RTG-3D sequence remains the assessment of myocardial fibrosis; hence the clinical applicability of this sequence to establish the relationship between epicardial fibrotic tissue and the anatomic path of coronary veins, which is clearly recognized in the literature as a critical factor in determining the success of CRT (22-24). The main objectives of CRT are to restore the coordination of myocardial contraction, thereby improving LVEF and causing reverse remodeling of the left ventricle. Despite the experience gained in the last 20 years,

it is still estimated that about 30-50% of patients undergoing CRT do not achieve the main objectives described (12, 13). Historically, the preferred method was to place the left ventricular (LV) lead in a lateral or posterolateral LV vein using intraprocedural DSA guidance. Current evidence has shown improved outcomes in terms of reducing treatment failure and heart failure-related hospitalizations by choosing the area with later activation and avoiding myocardial areas with fibrosis through CMR-guided CRT lead placement; this is supported by recent studies that reported CRT success rates of up to 93.1% when multimodality imaging pre-procedure planning is performed (18).

Another notable clinical setting where RTG-3D CMR could show its suitability occurs among patients with congenital heart disease, in whom they can not only accurately depict different features of distorted anatomy, but can also detect, delineate and quantify myocardial fibrosis, which is a commonly recognized entity in this subgroup of patients, and has been found to be associated with cardiac arrhythmias, altered ventricular mechanics and decreased functional status (25-27). This

work found accompanying myocardial fibrosis in one third of patients with congenital heart disease and thus provided additional information to physicians caring for those patients who in most cases were unaware of its presence.

In assessing the limitations of the study, the authors acknowledge the lack of internal comparison between the CMR findings of this cohort and the current gold standard, which is DSA, to validate visualization rates and to be able to calculate the individual sensitivity and specificity of each technique. Despite the consensus among those interpreting the images, another potential limitation is the lack of understanding of the intraobserver and interobserver correlation that the calculation of the kappa coefficient could serve as an additional validation tool for this type of study.

Finally, with the information obtained from this and other similar studies, lines of research should be pursued on adequate preprocedural assessment of CVA in patients undergoing CRT, in addition to adequate intraprocedural correlation and postprocedural follow-up.

Table 3. Comparison between available studies evaluating coronary venous anatomy

	Blendea et al. 2007 [^]	Chiribiri et al. 2008 [^]	Younger et al. 2009 [*]	Blanco et al. 2019 [*]
Study population= n	51	23	31	138
Technique	DSA	1.5T CMR sequence, RTG-3D	1.5T CMR sequence, RTG-3D	3T CMR sequence, RTG-3D
Reported visualization rates of coronary venous structures (%)				
Coronary sinus	100	100	100	100
Anterior Interventricular Vein	100	65	78	98.7
Posterior Interventricular Vein	76	96	83	96.2
Great Cardiac Vein	100	52	N/R	98.1
Lateral veins, left ventricle, including marginal and posterolateral veins	98	70	89	91.6
p-value+	N/A	N/A	<0.005	< 0.001

Notes: [^]: overall reported visualization rate; ^{*}: combined results of optimal and good quality groups; N/A: not evaluated, N/R: not reported; DSA: digital subtraction angiogram, +: Chi-square test.

Table 4. Comparison of visualization of coronary venous anatomy between DSA and 3 T CMR using RTG-3D

Structures Visualized	Blendea et al., 2007 (%) ASD	Blanco et al., 2019 (%) 3T RMC	p-value*
Coronary sinus	100	100	>0.999
Anterior interventricular vein	100	98.7	>0.999
Posterior interventricular vein	76	96.2	<0.001
Great cardiac vein	100	98.1	0.773
Lateral veins of the left ventricle. including marginal and posterolateral veins	98	91.6	0.178

Notes: *: p-value obtained by Fisher's exact test.

4. Conclusion

Assessment of non-invasive coronary venous anatomy is feasible with the RTG-3D sequence obtained in 3 T CMR, with which similar diagnostic performance is achieved compared to DSA venography. This approach may offer a valuable clinical tool for planning and monitoring electrophysiological procedures. Further studies are required to validate these findings.

List of acronyms

DSA: digital subtraction angiogram
 CTA: computed tomography angiography
 CVA: coronary venous anatomy
 LVEF: left ventricular ejection fraction
 GCV: great coronary vein
 CMR: cardiac magnetic resonance
 LGE: late gadolinium enhancement
 LGE-3D: three-dimensional late gadolinium enhancement
 CRT: cardiac resynchronization therapy
 AIV: anterior interventricular vein
 PIV: posterior interventricular vein
 MV: marginal vein
 PLV: posterolateral vein

Acknowledgments

To Diana Marcela Marín Pineda, statistician and epidemiologist, School of Medicine, Universidad Pontificia Bolivariana, Medellín, Colombia, for her advice on methodology and statistical analysis.

References

- Blendea D, Shah RV, Auricchio A, Nandigam V, Orencole M, Heist EK, et al. Variability of coronary venous anatomy in patients undergoing cardiac resynchronization therapy: A high-speed rotational venography study. *Hear Rhythm*. 2007;4(9):1155-62.
- Van de Veire NR, Marsan NA, Schuijff JD, Bleeker GB, Wijffels MCEF, van Erven L, et al. Noninvasive imaging of cardiac venous anatomy with 64-slice multi-slice computed tomography and noninvasive assessment of left ventricular dyssynchrony by 3-dimensional tissue synchronization imaging in patients with heart failure scheduled for cardiac re. *Am J Cardiol*. 2008;101(7):1023-9.
- Tada H, Kurosaki K, Naito S, Koyama K, Itoi K, Ito S, et al. Three-dimensional visualization of the coronary venous system using multidetector row computed tomography. *Circ J*. 2005;69(2):165-70.
- Echeverri D, Cabrales J, Jiménez A. Myocardial venous drainage: from anatomy to clinical use. *J Invasive Cardiol*. 2013;25(2):98-105.
- Nguyễn UC, Cluitmans MJM, Luermans JGLM, Strik M, de Vos CB, Kietselaer BLJH, et al. Visualisation of coronary venous anatomy by computed tomography angiography prior to cardiac resynchronisation therapy implantation. *Netherlands Hear J*. 2018;26(9):433-44.
- Mischke K, Knackstedt C, Mühlenthal G, Schimpf T, Neef P, Zarse M, et al. Imaging of the coronary venous system: Retrograde coronary sinus angiography versus venous phase coronary angiograms. *Int J Cardiol*. 2007;119(3):339-43.
- Nguyễn UC, Cluitmans MJM, Strik M, Luermans JG, Gommers S, Wildberger JE, et al. Integration of cardiac magnetic resonance imaging, electrocardiographic imaging, and coronary venous computed tomography angiography for guidance of left ventricular lead positioning. *Europace*. 2019;21(4):626-35. doi: 10.1093/europace/euy292.
- Abbara S, Cury RC, Nieman K, Reddy V, Moselewski F, Schmidt S, et al. Noninvasive evaluation of cardiac veins with 16-MDCT angiography. *AJR Am J Roentgenol*. 2005;185(4):1001-6.
- Młynarski R, Młynarska A, Sosnowski M. Anatomical variants of coronary venous system on cardiac computed tomography. *Circ J*. 2011;75(3):613-8.
- Malagò R, Pezzato A, Barbiani C, Sala G, Zamboni GA, Tavella D, et al. Non invasive cardiac vein mapping: role of multislice CT coronary angiography. *Eur J Radiol*. 2012;81(11):3262-9.
- Gene B, Solak A, Sahin N, Gur S, Kalaycioglu S, Ozturk V. Assessment of the coronary venous system by using cardiac CT. *Diagnostic Interv Radiol*. 2013;19(4):286-93.
- Behar JM, Mountney P, Toth D, Reiml S, Panayiotou M, Brost A, et al. Real-Time X-MRI-guided left ventricular lead implantation for targeted delivery of cardiac resynchronization therapy. *JACC Clin Electrophysiol*. 2017;3(8):803-14.
- Behar JM, Claridge S, Jackson T, Sieniewicz B, Porter B, Webb J, et al. The role of multi modality imaging in selecting patients and guiding lead placement for the delivery of cardiac resynchronization therapy. *Expert Rev Cardiovasc Ther*. 2017;15(2):93-107.
- Bakos Z, Markstad H, Ostenfeld E, Carlsson M, Rojter A, Borgquist R. Combined preoperative information using a bullseye plot from speckle tracking echocardiography, cardiac CT scan, and MRI scan: targeted left ventricular lead implantation in patients receiving cardiac resynchronization therapy. *Eur Heart J Cardiovasc Imaging*. 2014;15(5):523-31.
- Younger JF, Plein S, Crean A, Ball SG, Greenwood JP. Visualization of coronary venous anatomy by cardiovascular magnetic resonance. *J Cardiovasc Magn Reson*. 2009;11(1):26.
- Nguyễn UC, Mafi-Rad M, Aben J-P, Smulders MW, Engels EB, van Stipdonk AMW, et al. A novel approach for left ventricular lead placement in cardiac resynchronization therapy: Intra-procedural integration of coronary venous electroanatomic mapping with delayed enhancement cardiac magnetic resonance imaging. *Hear Rhythm*. 2017;14(1):110-9.
- Shetty AK, Duckett SG, Ginks MR, Ma Y, Sohal M, Bostock J, et al. Cardiac magnetic resonance-derived anatomy, scar, and dyssynchrony fused with fluoroscopy to guide LV lead placement in cardiac resynchronization therapy: a comparison with acute haemodynamic measures and echocardiographic reverse remodelling. *Eur Heart J Cardiovasc Imaging*. 2013;14(7):692-9.
- Kočková R, Sedláček K, Wichterle D, Šikula V, Tintěra J, Jansová H, et al. Cardiac resynchronization therapy guided by cardiac magnetic resonance imaging: A prospective, single-centre randomized study (RMC-CRT). *Int J Cardiol*. 2018;270:325-30.
- Heydari B, Jerosch-Herold M, Kwong RY. Imaging for planning of cardiac resynchronization therapy. *JACC Cardiovasc Imaging*. 2012;5(1):93-110.
- Chiribiri A, Kelle S, Götz S, Kriatselis C, Thouet T, Tangcharoen T, et al. Visualization of the cardiac venous system using cardiac magnetic resonance. *Am J Cardiol*. 2008;101(3):407-12.
- Younger JF, Plein S, Crean A, Ball SG, Greenwood JP. Visualization of coronary venous anatomy by cardiovascular magnetic resonance. *J Cardiovasc Magn Reson*. 2009;11(1):26.
- Khan FZ, Virdee MS, Palmer CR, Pugh PJ, O'Halloran D, Elvik M, et al. Targeted left ventricular lead placement to guide cardiac resynchronization therapy: the target study: a randomized, controlled trial. *J Am Coll Cardiol*. 2012;59(17):1509-18.
- Jin Y, Zhang Q, Mao J, He B. Image-guided left ventricular lead placement in cardiac resynchronization therapy for patients with heart failure: a meta-analysis. *BMC Cardiovasc Disord*. 2015;15(1):36.
- White JA, Yee R, Yuan X, Krahn A, Skanes A, Parker M, et al. Delayed enhancement magnetic resonance imaging predicts response to cardiac resynchronization therapy in patients with intraventricular dyssynchrony. *J Am Coll Cardiol*. 2006;48(10):1953-60.
- Rathod RH, Powell AJ, Geva T. Myocardial fibrosis in congenital heart disease. *Circ J*. 2016;80(6):1300-7.
- Ntsinjana HN, Hughes ML, Taylor AM. The role of cardiovascular magnetic resonance in pediatric congenital heart disease. *J Cardiovasc Magn Reson*. 2011;13(1):51.
- Tian J, An X, Niu L. Myocardial fibrosis in congenital and pediatric heart disease. *Exp Ther Med*. 2017;13(5):1660-4.

Correspondence

Natalia Sierra
 Universidad CES
 Calle 6A # 16-15, apto. 602
 Medellín, Colombia
 sierrisna@hotmail.com

Received for evaluation: November 15, 2021
 Accepted for publication: February 10, 2022